



# Exploiting second-order advantage from mathematically modeled voltammetric data for simultaneous determination of multiple antiparkinson agents in the presence of uncalibrated interference

Ghobad Mohammadi<sup>a</sup>, Khodabakhsh Rashidi<sup>b</sup>, Majid Mahmoudi<sup>b</sup>, Hector C. Goicoechea<sup>c</sup>, Ali R. Jalalvand<sup>b,\*</sup>

<sup>a</sup> Department of Pharmaceutics, School of Pharmacy, Kermanshah University of Medical Sciences, Kermanshah, Iran

<sup>b</sup> Research Center of Oils and Fats, Kermanshah University of Medical Sciences, Kermanshah, Iran

<sup>c</sup> Laboratorio de Desarrollo Analítico y Quimiometría (LADAQ), Catedra de Química Analítica I, Universidad Nacional del Litoral, Ciudad Universitaria, CC242 (S3000ZAA), Santa Fe, Argentina

## ARTICLE INFO

### Article history:

Received 1 February 2018

Revised 21 March 2018

Accepted 5 April 2018

Available online 25 April 2018

### Keywords:

Antiparkinson agents

Multi-way calibration

Second-order advantage

Simultaneous determination

Uncalibrated interference

## ABSTRACT

In this work, we are going to develop an efficient electroanalytical methodology based on generation of second-order differential pulse voltammetric (DPV) data at different pulse heights to exploit second-order advantage for simultaneous determination of levodopa (LDP), carbidopa (CDP), methyl dopa (MDP), benserazide (BA), tolcapone (TOL) and entacapone (ENT) in the presence of dopamine (DPA) as uncalibrated interference. The recorded data were baseline- and potential shift-corrected by asymmetric least square spline regression (AsLSSR) and correlation optimized warping (COW) algorithms, respectively. After data pre-processing, multivariate curve resolution-alternating least squares (MCR-ALS) and parallel factor analysis 2 (PARAFAC2) were used to develop three-way calibration models and then, the abilities of the developed models to predict analytes' concentrations in the absence and presence of DPA were examined in validation and test sets, respectively. MCR-ALS acted better than PARAFAC2 to predict analytes' concentrations in the absence and presence of DPA as uncalibrated interference. Therefore, MCR-ALS was chosen to predict antiparkinson agents' concentrations in spiked human serum samples as real cases. Fortunately, acceptable results were obtained which were comparable to those obtained by high performance liquid chromatography with UV detection (HPLC-UV) as reference method.

© 2018 Taiwan Institute of Chemical Engineers. Published by Elsevier B.V. All rights reserved.

## 1. Introduction

Parkinson's disease (PD) which mainly affects the motor system is a degenerative disorder of the central nervous system [1,2]. The PD can cause rigidity, depression, anxiety, shaking, thinking and behavioral problems, slowness of movement and difficulty with walking. The PD is caused by a significant decrease at the dopamine (DPA) neurotransmitter level in the brain [1]. The PD has no cure, but medications can save the patient from the symptoms in some extent. The most important drugs which are useful to treat the PD are divided into three groups including levodopa (LDP), DPA agonists and monoamine oxidase B inhibitors [1]. The LDP has been widely used to treat the PD which is converted to DPA by the dopa decarboxylase in the dopaminergic neurons. Carbidopa (CDP) is another drug given to patients with PD in order to inhibit peripheral metabolism of LDP [3]. This property is important for central nervous system effect because allows a larger amount of peripheral LDP to cross the blood-brain barrier. The LDP in combination with CDP is used to improve motor function in

**Abbreviations:** PD, Parkinson's disease; DPA, dopamine; LDP, levodopa; carbidopa, CDP; MDP, methyl dopa; BA, benserazide; TOL, tolcapone; ENT, entacapone; COMT, catechol-O-methyltransferase; HPLC-DAD, high performance liquid chromatography with diode array detection; LC-ATR-FTIR, liquid chromatography-attenuated total reflectance-Fourier transform infrared spectroscopy; LC-DAD-MS, liquid chromatography-diode array detection-mass spectrometry; FIA-DAD, flow injection analysis-diode array detection; COW, correlation optimised warping; AFOM, analytical figure of merit; NAS, net analyte signal; LOD, limit of detection; DPV, differential pulse voltammetry; CV, cyclic voltammetry; SCCD, small central composite design; MCR-ALS, multivariate curve resolution alternating least squares; PARAFAC2, parallel factor analysis 2; AsLSSR, asymmetric least squares spline regression; COW, correlation optimised warping; RMSEP, root mean square error of prediction; REP, relative error of prediction; PARAFAC, parallel factor analysis; PBS, phosphate buffered solution; DDW, doubly distilled water; AFOM, analytical figure of merit; lof, lack of fit; GE, gold electrode.

\* Corresponding author.

E-mail address: [ali.jalalvand1984@gmail.com](mailto:ali.jalalvand1984@gmail.com) (A.R. Jalalvand).

the patients with the PD [4], however, treatment with LDP/CDP causes several untoward effects [5]. Methyldopa (MDP) is a major metabolite of LDP and its elevated blood levels are associated with the occurrence of LDP-induced dyskinesias in patients with the PD. Some research groups have claimed that the MDP levels or MDP/LDP ratios in human plasma can be used as predictive indicators of the long-term response to LDP therapy [6,7]. Benserazide (BA) is a dopa decarboxylase inhibitor which in combination with LDP is used to manage the PD [8]. Tolcapone (TOL) with commercial name "Tasmar" is a selective nitrocatechol-type inhibitor of the enzyme catechol-O-methyltransferase (COMT) which is used to treat the PD [9]. Entacapone (ENT) with the commercial name "Comtan" is a drug which commonly in combination with other medications is used to treat the PD [10]. Application of the medications to cure the PD affects the DPA levels therefore, DPA must be also determined when the anti-Parkinson drugs are used. Therefore, DPA can be regarded as an uncalibrated interference in determination of the drugs mentioned above. Generally, these medications are determined separately or simultaneously by chromatographic methods which are too expensive and time-consuming. Therefore, developing novel analytical methods for determination of these drugs which are fast and low-cost is highly required.

Multi-way calibration which acts based on several instrumental signals per sample is organized into a mathematical object with more modes than a vector, e.g., as a data matrix [11,12]. The most important practical aspect of multi-way calibration is determination of the analyte(s) of interest in the presence of uncalibrated interference, this property is known as second-order advantage. Multi-way calibration increases the sensitivity due to the measurement of redundant data which decreases the relative impact of the noise in the data and selectivity is also increased because each new instrumental mode contributes positively to the overall selectivity [13,14]. Furthermore, multi-way calibration enables the analytical chemist to obtain more qualitative information about the chemical phenomena than with univariate or first-order data. Several techniques such as fluorescence excitation-emission [15], high performance liquid chromatography with diode array detection (HPLC-DAD) [16], liquid chromatography-attenuated total reflectance-Fourier transform infrared spectroscopy (LC-ATR-FTIR) [17], liquid chromatography-DAD-mass spectrometry (LC-DAD-MS) [18], flow injection analysis-DAD (FIA-DAD) [19], DAD-kinetics [20] and pH-DAD [21] have been used to obtain second-order data. Although these techniques are accurate and reliable but suffer from several disadvantages such as high-cost and complexity of their instruments. Therefore, new techniques are highly required for the inexpensive quantification of analytes in complex matrices. Among the available analytical methods, electrochemical methods with low-cost instruments and applicability to miniaturization are a good choice for accurate, fast and reliable determination of the analyte(s) of interest in interfering media [22–28]. The use of chemometrics in analytical electrochemistry was scarce for many years in comparison to the other techniques especially spectroscopic techniques and this may be related to the lack of linearity between the current and concentration. But, development of non-linear methods and pre-processing methods have increased applications of chemometrics to analytical electrochemistry during the last years [29–35].

In this study, we are going to record second-order differential pulse voltammetric (DPV) data at different pulse heights which help us to obtain three-way voltammetric data arrays for calibration model building by multivariate curve resolution-alternating least squares (MCR-ALS) and parallel factor analysis 2 (PARAFAC2). The developed calibration models will be used to predict concentrations of six anti-Parkinson agents in validation samples and after evaluating their performance, they will be applied to predict concentrations of anti-Parkinson agents in the presence of dopamine

(DPA) as uncalibrated interference to choose the best algorithm for the analysis of human serum samples. Finally, the results of the best algorithm applied to the analysis of serum samples will compared with those of obtained by high performance liquid chromatography with UV detection (HPLC-UV) as reference method. The schematic representation of the methodology developed in his work is shown in Scheme 1.

## 2. Theoretical and experimental considerations

### 2.1. Theoretical considerations

#### 2.1.1. Recording second-order DPV data

In our work, the pulse height as an instrumental parameter in DPV method was changed for obtaining second-order DPV data. Here, a brief description of the mathematical aspects of the proposed procedure will be given. The signal intensity in DPV can be described by the use of following equations [36]:

$$\delta_i = \frac{nFAD_0^{1/2}C_0^*}{\pi^{1/2}(\tau - \tau')^{1/2}} \left[ \frac{P_A(1 - \sigma^2)}{(\sigma + P_A)(1 + P_A\sigma)} \right] \quad (1)$$

$$P_A = \xi \exp \left[ \frac{nF}{RT} \left( E + \frac{\Delta E}{2} - E^0 \right) \right] \quad (2)$$

$$\sigma = \exp \left( \frac{nF}{RT} \frac{\Delta E}{2} \right) \quad (3)$$

$$\xi = \left( \frac{D_O}{D_R} \right)^{1/2} \quad (4)$$

where,  $\Delta E$  is referred to the pulse height,  $\tau$  is referred to pulse duration and other symbols are well-known and have their conventional meanings. For an electrochemical reaction, a vector can be produced by scanning the potential at constant  $\Delta E$  and  $\tau$ . Different data vectors can be produced by applying different  $\Delta E$ s and scanning the potential at the constant  $\tau$ . Therefore, by sweeping the potential and applying different  $\Delta E$ s at a constant  $\tau$  non-bilinear second-order DPV data will be obtained.

#### 2.1.2. Second-order algorithms

MCR-ALS: The theory of MCR-ALS is based on that the overall voltammetric landscape for a sample could be decomposed into the concentration profile and voltammograms of the species [37]. This means that MCR-ALS is able to separate the corresponding voltammetric landscape of two analytes with overlapping signals into the concentration profile and voltammograms for the two chemical species. Mathematically, if  $\mathbf{X}$  is an unfolded three-dimensional data array, it can be decomposed into two matrices containing the concentration profile and voltammograms of the species,  $\mathbf{C}$  and  $\mathbf{V}$ , respectively, according to:

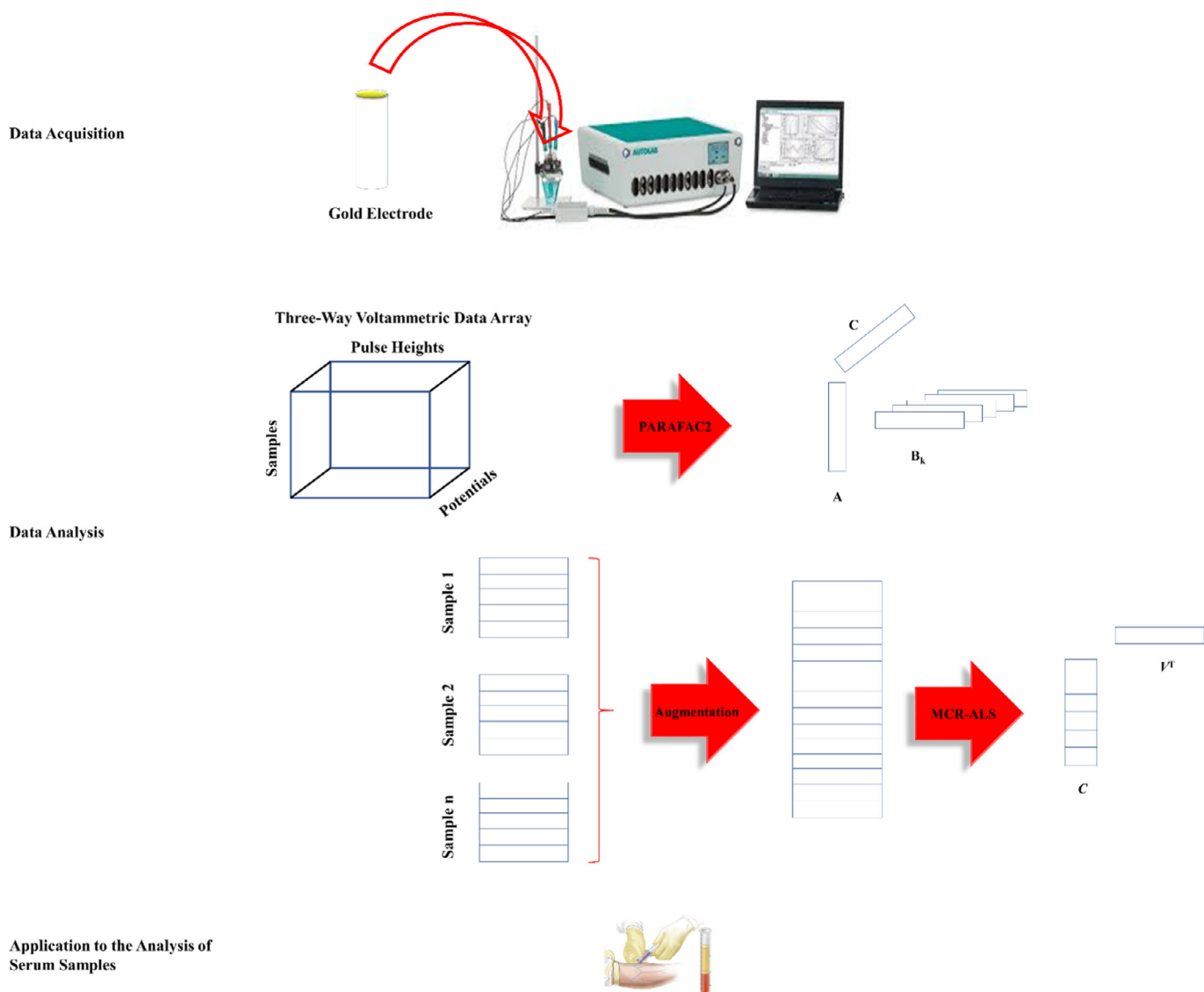
$$\mathbf{X} = \mathbf{CV}^T + \mathbf{E} \quad (5)$$

where  $\mathbf{E}$  is a residual matrix and its iterative least squares minimization is used as a criterion for decomposition of matrix  $\mathbf{X}$ . Here, a column-wise augmented matrix is created by unfolding a three-dimensional data array along the pulse height mode. This could be performed by placing sample matrix and the unknown matrix on top of each other [37]. Decomposition is started by supplying the estimated voltammograms of the various species which is applied to estimate  $\hat{\mathbf{C}}$ :

$$\hat{\mathbf{C}} = \mathbf{XV}^{T+} \quad (6)$$

where '+' refers to the pseudo-inverse. Then,  $\mathbf{V}$  will be re-estimated according to the Eq. (7):

$$\mathbf{S} = (\hat{\mathbf{C}} + \mathbf{X})^T \quad (7)$$



**Scheme 1.** Schematic representation of the methodology developed in this study to determine concentrations of six anti-Parkinson agents in the presence of DPA as uncalibrated interference.

Finally,  $\mathbf{E}$  could be calculated from Eq. (5) using  $\mathbf{X}$ ,  $\hat{\mathbf{C}}$  and  $\mathbf{V}$ . These steps under suitable constraints during the ALS optimization will be repeated until convergence is achieved. Finally, concentration profiles containing information can be used for quantitative predictions. In this approach the area under curve is proportional to concentration which could be applied to build a pseudo-univariate calibration curve.

**PARAFAC2:** The parallel factor analysis (PARAFAC) implies that all the contribution to the signal including analytes, interferents and background could be modeled by an individual component having the same concentration and voltammogram profiles along all the analysed samples (trilinearity). In mathematical points of view, if  $\mathbf{X}$  is a three-way data array corresponding to the measurement of the voltammetric landscapes on different samples, it could be decomposed into sample ( $\mathbf{A}$ ), pulse height ( $\mathbf{B}$ ) and voltammogram ( $\mathbf{C}$ ) loadings according to:

$$\mathbf{X} = \mathbf{A}(\mathbf{C}|\otimes|\mathbf{B})^T \quad (8)$$

where  $\mathbf{X}$  is the unfolded  $\mathbf{X}$  and  $|\otimes|$  is a column-wise Kronecker product of the two matrices. When the loadings along the  $\mathbf{A}$  are linearly proportional to components' concentrations the trilinearity

assumption holds and can be applied to calibration. However, for voltammetric data in the presence of shifts and shape changes the trilinearity structure is disrupted which makes the PARAFAC model inappropriate. PARAFAC2 is a more flexible variant of PARAFAC which handles shifts and changes in peak shapes by regarding a different set of loadings for samples [38–40]. In this case, a modified version of Eq. (8) is:

$$\mathbf{X}_k = \mathbf{A}_k \mathbf{C}_k \mathbf{B}_k^T \quad (9)$$

where  $\mathbf{X}_k$  is the voltammetric landscape measured for the  $k$ th sample,  $\mathbf{A}_k$  is a diagonal matrix containing elements the  $k$ th row of the matrix  $\mathbf{A}$ , and  $\mathbf{B}_k$  is the pulse height loading matrix estimated for the  $k$ th sample. As for PARAFAC, the solution used is unique which is necessary for handling complex overlapping signals.

### 2.1.3. Data pre-processing

**Baseline correction:** Baseline elimination is a critical step which enhances the signals and reduces the complexity of the analytical data [41,42]. Therefore, we applied the methodology proposed by Eilers et al. for baseline correction based on asymmetric least squares splines regression approach (AsLSSR). In their method the

following function is minimized:

$$Q = \sum_i v_i (y_i - f_i)^2 + \lambda \sum_i (\Delta^2 f_i)^2 \quad (10)$$

where  $y$  is the recorded signal,  $f$  is an approximation of the baseline trend ( $y$ ),  $\Delta$  is the derivative of  $f$ ,  $i$  is successive values of the signal,  $\lambda$  is the regularization parameter and  $v$  includes weights. The positive and negative deviations from the estimated baseline have low and high values of  $v$ , respectively. The method proposed by Eilers et al. uses spline basis functions to estimate a two dimensional background matrix  $\mathbf{B}$ . To increase the speed of calculation and accuracy of the results, 10 basis functions with a single  $\lambda$  with the value equal to one were used in this study. Details of the mentioned method can be found in the literature [41,42].

**2.1.3.2. Potential shift correction.** Linearity is a property which is needed for the application of linear multivariate calibration algorithms [34,35]. However, in many situations such as interactions between individual components deviations from the linearity can be observed. Generally, nonlinearity causes signal shifts, broadening of the peak and some non-proportional increase in the peak intensity. Such problems become more important in the presence of signal overlapping. These effects hinder the direct application of linear multivariate calibration algorithms and must be tackled. Therefore, data alignment is a crucial step which must be performed before application of linear multivariate calibration algorithms. The data alignment techniques act based on digital moving (and/or stretching or compressing) a voltammogram towards a reference one and the quality of matching is guaranteed with certain objective functions such as residual fit, correlation coefficient, similarity index, etc.

In this study, correlation optimised warping (COW) algorithm was applied to potential shift correction.

The COW is a piecewise or segmented data preprocessing method aimed at aligning a sample data vector towards a reference vector by allowing limited changes in segments lengths on the sample vector [43–45]. To more understand about details of the COW, the reader is referred to Refs. [43–45].

#### 2.1.4. Model efficiency estimation

To understand whether a developed model can be applied for the analysis of real samples or not, model validation is must be performed. In order to achieve this goal, each model was applied to validation set and its results were examined by evaluating root mean square errors of prediction (RMSEP), and relative error of prediction (REP) according to the following definitions:

$$RMSEP = \sqrt{\frac{\sum_{i=1}^n (y_{pred} - y_{act})^2}{n}} \quad (11)$$

$$REP(\%) = \frac{100}{y_{mean}} \sqrt{\frac{1}{n} \sum_{i=1}^n (y_{pred} - y_{act})^2} \quad (12)$$

where  $y_{act}$  and  $y_{pred}$  are nominal and predicted concentrations, respectively, and  $y_{mean}$  is the mean of the nominal concentrations.  $m$  and  $n$  refer to the number of samples used for building calibration and validation sets, respectively.

#### 2.1.5. Analytical figures of merit for comparing performance of PARAFAC2 and MCR-ALS

An analytical figure of merit (AFOM) is a quantity which is used to verify the performance of an analytical method. In analytical calibration, the AFOMs are used to compare the performances and detection capabilities of different analytical methods [46].

In multi-way calibration and particularly in three-way calibration, there are several protocols for determination of the sensitivity and some of these protocols are based on extensions of the net analyte signal (NAS) concept from first-order to second-order [46]. These approaches are faced to some difficulties such as different NAS definitions which depend on the way of applying the NAS concept and extrapolation of these expressions to higher-order data which hinders a significant underestimation of the sensitivity. Fortunately, there is an alternative approach to estimate sensitivity which is based on the relation of output to input noise [46]. More sensitivity is obtained if large input noise leads to small output noise according to the following definition:

$$\text{Sensitivity} = \sigma_x / \sigma_y \quad (13)$$

where  $\sigma_x$  and  $\sigma_y$  define the uncertainties of signal and concentration, respectively [46].

According to IUPAC definition, selectivity is a quantity which estimates the capability of a method for determination of particular analytes in mixtures without interferences from other components [46]. In three-way calibration selectivity can be defined as the ratio between the sensitivity and the slope of the pseudo-univariate calibration graph according to the following definition:

$$\text{Selectivity} = \text{Sensitivity} / S_n \quad (14)$$

The level of overlapping among the profiles of different components determines the value by which SEN departs from  $S_n$ .

Sensitivity depends on the type of signal employed to develop a calibration method therefore, sensitivities derived from different types of measurements cannot be compared on an equal basis. For this reason, analytical sensitivity is proposed and is defined as the ratio between sensitivity and instrumental noise:

$$\text{Analytical Sensitivity} = \text{Sensitivity} / \sigma_x \quad (15)$$

where  $\sigma_x$  is an estimation of noise level in measured signals. The unit of analytical sensitivity is concentration<sup>-1</sup> and is independent on the signal. Therefore, analytical sensitivity can be used to compare methodologies based on very different instrumental measurements.

The inverse of analytical sensitivity reports the minimum concentration difference between two samples which the model is able to determine it. Finally, according to Eq. (16) the limit of detection (LOD) can be defined as 3.3 times the standard deviation for the blank sample:

$$LOD = 3.3S_b \quad (16)$$

## 2.2. Experimental considerations

### 2.2.1. Chemicals and solutions

LDP, CDP, MDP, BA, TOL, ENT and DPA were prepared from Sigma-Aldrich. The phosphate buffered solution (PBS, 0.05 M) was prepared from  $\text{NaH}_2\text{PO}_4$  and  $\text{Na}_2\text{HPO}_4$  and its pH was adjusted using appropriate amounts of NaOH and  $\text{H}_3\text{PO}_4$ . All other chemicals used in this work were of analytical grade and purchased from well-known companies. Stock standard solutions of LDP, CDP, MDP, BA, TOL, ENT and DPA with a concentration level of 0.1 M were prepared by dissolution of exact amounts of their solid powders in the PBS (0.05 M, pH 2) and stored in a refrigerator. Working solutions of the medications were prepared by appropriate dilution of their stock solutions with PBS (0.05 M, pH 2). All the solutions used in this study were prepared by doubly distilled water (DDW).

### 2.2.2. Instruments and softwares

Electrochemical data acquisition was performed by an Autolab PGSTAT302N-High Performance controlled by the NOVA software (Version 2.1) and equipped by a conventional cell with an Ag/AgCl as reference electrode, a Pt wire as auxiliary electrode

and a gold electrode (GE, Metrohm, disk material = gold, disk diameter = 5 mm, length = 52.5 mm) as working electrode. pH adjustments were performed by a professional waterproof portable pH/ORP meter (Hanna Instruments) equipped by a combined glass electrode. HPLC analyses were carried out by a HPLC system consisted of a Younglin ACME 9000.0 equipped with a quaternary pump, online degasser, column heater, autosampler and UV detector. Data collection and analyses were performed using Autochro 2000.0 software (Younglin). Separation was achieved on C-18 column, Perfectsil Target ODS3 (150.0 mm × 4.6 mm, 5.0 μm) with a 10.0 mm × 4.0 mm, 5.0 μm guard column (MZ-Analysentechnik, Mainz, Germany). The mobile phase consisted of acetate-citrate buffer containing sodium acetate (0.05 M), citric acid monohydrate (10 mM), octanesulphonic acid (0.5 mM), Na<sub>2</sub>EDTA (0.05 mM) and dibutylamine (0.5 mM). The flow-rate was set at 1 mL min<sup>-1</sup>. The recorded electrochemical data was transformed into the MATLAB environment (Version 7.14, MathWorks, Inc.) for pre-processing (smoothing, baseline- and potential-shift corrections) and multi-way analyses. All the computations were performed on a personal DELL XPS laptop (L502X).

### 2.2.3. Preparation of real samples

A human serum sample was provided by a Medical Diagnostic Laboratory in Kermanshah, Iran. A methodology reported by the other researchers was applied to prepare the serum samples for the analysis [47]. According to their method, 10.0 mL of the serum sample was transferred into a glass tube containing 10.0 mL of 15.0% (w/v) zinc sulfate-acetonitrile (50/40,v/v) and vortexed for 30.0 min. The glass tube was kept at 4.0 °C for 15.0 min and subsequently centrifuged at 5000.0 rpm for 5.0 min. Finally, the supernatant was discarded and the solution was used for next analyses. The serum samples were partially diluted with PBS (0.05 M, pH 2) and spiked with randomly selected amounts of LDP, CDP, MDP, BA, TOL, ENT and DPA. Then, aliquots of the diluted samples were injected into the electrochemical cell for quantitative purposes.

### 2.2.4. Electrochemical procedure

Prior to electrochemical measurements, the GE was well polished by a silky pad and 0.05 μm alumina slurry. Afterward, the GE was washed by ethanol and DDW and left to be dried at room temperature. All electrochemical data was recorded at room temperature. The second-order DPV data was recorded according to the following operating conditions: step potential 0.005 V, pulse heights 0.2, 0.15, 0.10, 0.05 and 0.025 V, modulation time 0.05 s and interval time 0.5 s.

## 3. Results and discussion

### 3.1. Selecting the best pH

For selecting the best pH for the simultaneous determination of LDP, CDP, MDP, BA, TOL and ENT, the effect of pH on their cyclic voltammograms (CVs) was investigated. Fig. 1A–F shows the CVs of LDP, CDP, MDP, BA, TOL and ENT recorded in the PBS (0.05 M) at different pHs in the range of 2.0–12.0. As can be observed in Fig. 1A–F, all CVs of the studied drugs have a maximum current at pH 2. From analytical point of view both maximal and stable signals are preferable therefore, a pH value of 2.0 was selected for next experiments.

### 3.2. Chemometric investigations

#### 3.2.1. Understanding the necessity of multi-way calibration

Fig. 2 shows the CVs of LDP (curve a), CDP (curve b), MDP (curve c), BA (curve d), TOL (curve e), ENT (curve f) and DPA (curve

g) in PBS (0.05 M, pH 2). As can be seen, a strong signal overlapping could be observed for the simultaneous analysis of LDP, CDP, MDP, BA, TOL and ENT in the presence of DPA at the GE. Therefore, determination of any of these drugs will be biased if univariate calibration is applied as the analytical method, and for shooting this trouble it is necessary to use multi-way calibration. Since DPV is much higher sensitive than CV, it will be used to simultaneous determination of the studied drugs.

#### 3.2.2. Calibration procedures

**Univariate calibrations:** Prior to multi-way calibration, univariate calibration curves were constructed based on DPV method using several points as peak current versus drug concentration and evaluated by linear regression (Fig. 3). All drugs showed a linear dependence between peak current and concentration at different concentrations intervals LDP (1.0–20.0 μM and 20.0–320.0 μM), CDP (0.5–600.0 μM), MDP (2.0–32.0 μM and 32.0–380.0 μM), BA (1.0–36.0 μM), TOL (0.1–14.0 μM and 14.0–178.0 μM) and ENT (2.0–85.0 μM), (see insets of Fig. 3).

**Calibration set:** A calibration set including thirty three mixtures in which compositions of the mixtures were selected according to a small central composite design (SCCD, Table 1) was prepared in the PBS (0.05 M, pH 2) spiked with appropriate amounts of drugs considering their linear calibration ranges obtained from univariate calibrations. The prepared mixtures were transferred into the electrochemical cell in random order and their voltammograms were recorded.

**Validation set:** To verify the prediction ability of the developed calibration models after optimizing all calibration parameters, a validation set including ten mixtures (Table 1) was prepared in the PBS (0.05 M, pH 2) spiked with randomly selected concentration of LDP, CDP, MDP, BA, TOL and ENT from their corresponding calibration ranges. All samples were transferred into the electrochemical cell and their voltammograms were registered.

**Test set:** With the aim of evaluating performance of the developed calibration model to predict concentrations of LDP, CDP, MDP, BA, TOL and ENT in the presence of DPA as uncalibrated interference, a test set involving ten mixtures was prepared in the PBS (0.05 M, pH 2) with random concentrations of the drugs in the same concentration range used for building the calibration set (Table 1). All samples were transferred into the electrochemical cell and their voltammograms were registered in random order.

#### 3.2.3. Data pretreatment

It has been proven by the previous studies that the performance of voltammetric methods can be enhanced by data pretreatments [29–35]. In the present study, besides the overlapping challenge, there are two additional problems including: (1) the baselines of the signals, and (2) sample-to-sample potential-shifts which are common problems in voltammetric measurements. For tackling the baseline challenge, it is necessary to eliminate the baselines by baseline correction. Regarding the second challenge, the potentials shifts were corrected by COW algorithm as an efficient chemometric technique. For more understanding about the details of the baseline- and potential shift-correction techniques the reader is referred to Refs. [29–35].

Regarding the problems mentioned above, the matrices related to the raw data (Fig. 4) were placed next to each other to obtain an expanded matrix which was submitted to baseline correction and potential shift correction by AsLSSR and COW, respectively. Then, the pretreated data (baseline- and potential shift-corrected data) was mathematically assembled in MATLAB environment using the existing commands to restore their original format and used for next computations.

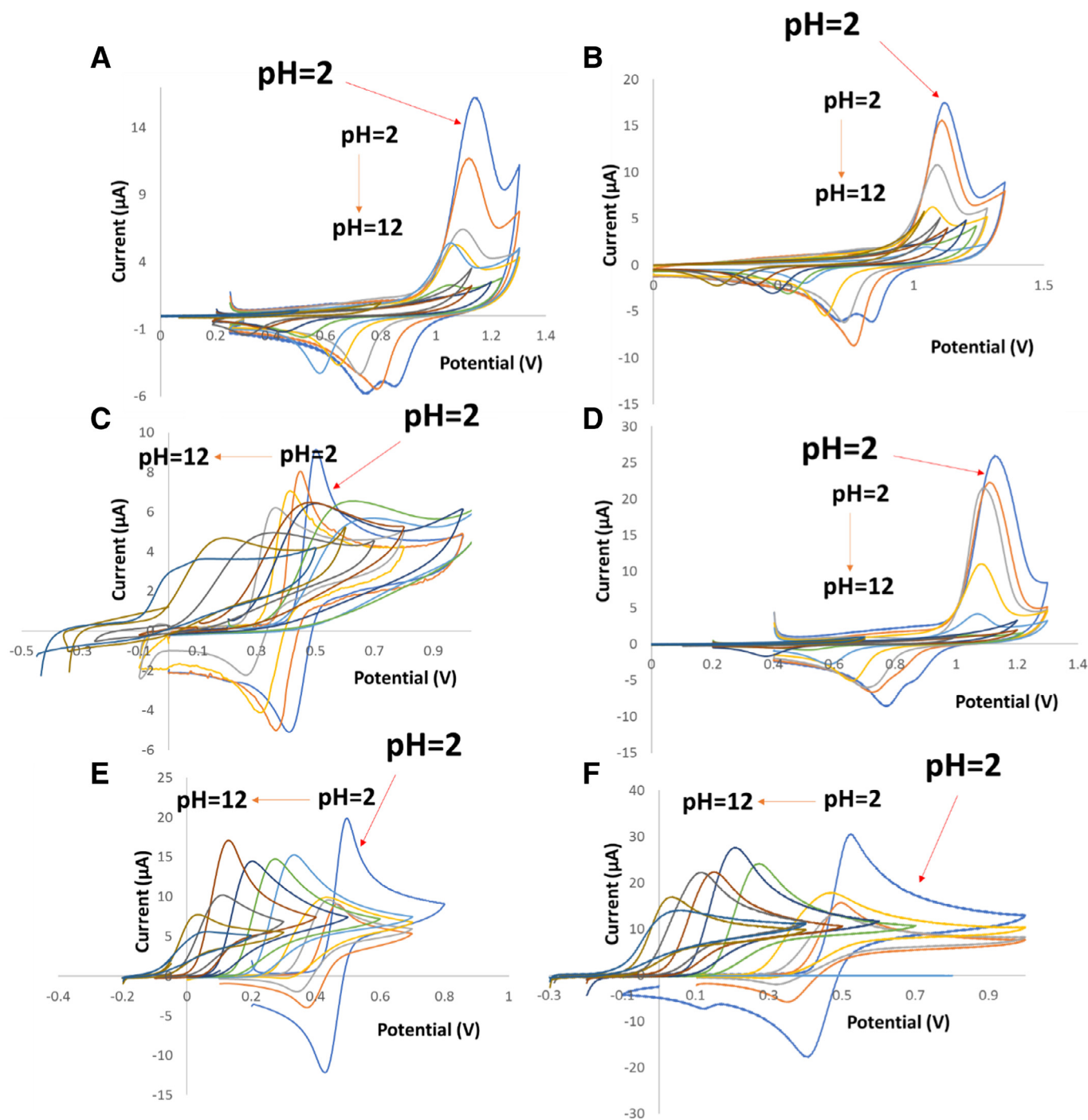


**Fig. 1.** Cyclic voltammograms of (A) LDP (1 mM), (B) CDP (1 mM), (C) MDP (1 mM), (D) BA (1 mM), (E) TOL (1 mM) and (F) ENT in PBS 0.05 M at different pHs.

### 3.3. Application of MCR-ALS and PARAFAC2 to the second-order data

#### 3.3.1. MCR-ALS modeling

The main premise of MCR techniques is to follow Beer's law. Consequently, they are able to analyze the bilinear data. Application of MCR-ALS to resolve data needs the uniform presentation of data, *i.e.*, all the signals must have the same length and corresponding variables must be placed into the proper columns of the data matrix. The voltammetric signals often do not fulfill this property and this problem is seen as the potential shift in voltammetric data. Potential shift causes a decrease in the linearity which depends on its magnitude. The lack of linearity can produce large

lack of fit (*lof*) values and hinders achievement of convergence and obtaining reliable results therefore, the results of MCR-ALS analysis are not satisfactory. As a result, the shift of potential in voltammetric data as a possible source of inefficiency must be corrected. Although the potential shift correction can tackle the non-bilinearity problem, it can produce rank deficient data. Thus, matrix augmentation can overcome the rank deficiency problem. According to results mentioned above, potential shift correction was performed for tackling the non-linearity and then, potential shift corrected data were augmented for the analysis by MCR-ALS. By the first attempt, MCR-ALS was applied to model the dataset and resolving the overlapping peaks into their components. In order to do this

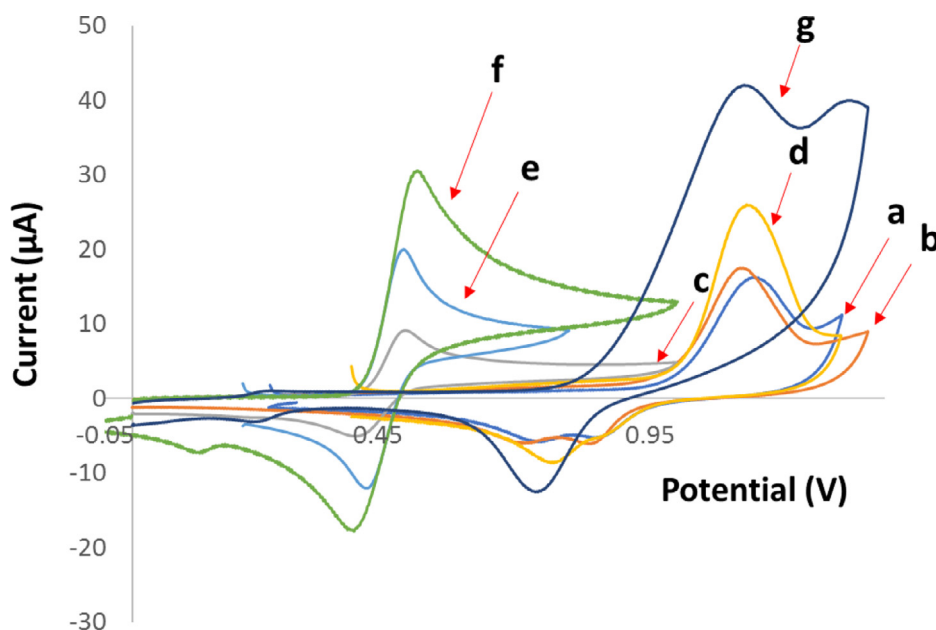


Fig. 2. Cyclic voltammograms of (a) LDP, (b) CDP, (c) MDP, (d) BA, (e) TOL, (f) ENT and (g) DPA in PBS (0.05 M, pH 2). Concentration of each drug is 1 mM.

**Table 1**  
Concentration data of calibration set ( $C_1$ – $C_{33}$ ), validation set ( $V_1$ – $V_{10}$ ), and test set ( $T_1$ – $T_{10}$ ).

Sample	LDP ( $\mu\text{M}$ )	CDP ( $\mu\text{M}$ )	MDP ( $\mu\text{M}$ )	BA ( $\mu\text{M}$ )	TOL ( $\mu\text{M}$ )	ENT ( $\mu\text{M}$ )	Sample	LDP ( $\mu\text{M}$ )	CDP ( $\mu\text{M}$ )	MDP ( $\mu\text{M}$ )	BA ( $\mu\text{M}$ )	TOL ( $\mu\text{M}$ )	ENT ( $\mu\text{M}$ )	DPA ( $\mu\text{M}$ )
$C_1$	320	0.5	380	1	178	85	$V_1$	260	15	55	20	5.5	50	–
$C_2$	1	600	380	36	0.1	85	$V_2$	300	24	60	12	24	45	–
$C_3$	160.5	300.25	191	18.5	89.05	85	$V_3$	180	150	45	10	33	21	–
$C_4$	320	0.5	2	36	0.1	2	$V_4$	11	121	33	5	12	11	–
$C_5$	1	600	2	1	178	2	$V_5$	20	133	21	8	6	31	–
$C_6$	160.5	300.25	191	36	89.05	43.5	$V_6$	6	90	42	15	66	12	–
$C_7$	1	600	380	1	0.1	2	$V_7$	244	85	31	22	75	8.6	–
$C_8$	160.5	300.25	191	18.5	0.1	43.5	$V_8$	310	54	29	5	9	25	–
$C_9$	1	600	2	36	178	85	$V_9$	180	33	23	28	3.5	41	–
$C_{10}$	160.5	300.25	191	18.5	89.05	43.5	$V_{10}$	100	22	35	11	18	50	–
$C_{11}$	320	600	2	36	178	2								
$C_{12}$	160.5	300.25	191	18.5	178	43.5								
$C_{13}$	160.5	600	191	18.5	89.05	43.5	$T_1$	98	50	60	35	41	15	180
$C_{14}$	160.5	300.25	191	1	89.05	43.5	$T_2$	88	80	58	20	29	25	160
$C_{15}$	320	600	2	1	178	85	$T_3$	77	90	45	18	54	31	220
$C_{16}$	1	0.5	2	36	0.1	85	$T_4$	200	100	54	22	4.6	28	270
$C_{17}$	1	0.5	380	36	178	85	$T_5$	300	149	33	34	11	55	280
$C_{18}$	1	300.25	191	18.5	89.05	43.5	$T_6$	210	54	22	30	38	44	250
$C_{19}$	160.5	300.25	191	18.5	89.05	43.5	$T_7$	220	33	50	15	80	21	300
$C_{20}$	160.5	300.25	191	18.5	89.05	43.5	$T_8$	280	22	48	10	20	18	219
$C_{21}$	1	0.5	2	1	0.1	2	$T_9$	144	79	31	8	10	43	290
$C_{22}$	1	0.5	380	1	178	2	$T_{10}$	233	88	30	14	5	53	300
$C_{23}$	320	0.5	380	36	178	2								
$C_{24}$	160.5	300.25	191	18.5	89.05	43.5								
$C_{25}$	160.5	300.25	380	18.5	89.05	43.5								
$C_{26}$	160.5	300.25	2	18.5	89.05	43.5								
$C_{27}$	320	300.25	191	18.5	89.05	43.5								
$C_{28}$	160.5	300.25	191	18.5	89.05	2								
$C_{29}$	320	600	380	1	0.1	85								
$C_{30}$	160.5	0.5	191	18.5	89.05	43.5								
$C_{31}$	320	0.5	2	1	0.1	85								
$C_{32}$	320	600	380	36	0.1	2								
$C_{33}$	160.5	300.25	191	18.5	89.05	43.5								

step, voltammetric landscapes recorded on the samples of the calibration set, each of them with size of  $(175 \times 5)$ , were collected into an unfolded two-way dataset in a column-wise augmentation manner by putting each matrix on top of the other. Therefore, a new  $5775 \times 5$  matrix was obtained which was submitted to the MATLAB workspace for the analysis by MCR-ALS. This algorithm requires initialization with system parameters as close as possible to the final results. Therefore, voltammograms of analytes

and interference are required owing that the resolution is based on the selectivity in the latter mode. In this work, the selection of the purest voltammogram for the interferent was made based on simple interactive self-modeling mixture analysis (SIMPLISMA) [48]. The number of contributing components in the studied system was determined based on singular value decomposition (SVD) and six components were found when analyzing validation samples. Then, a model including six components, one for each analyte

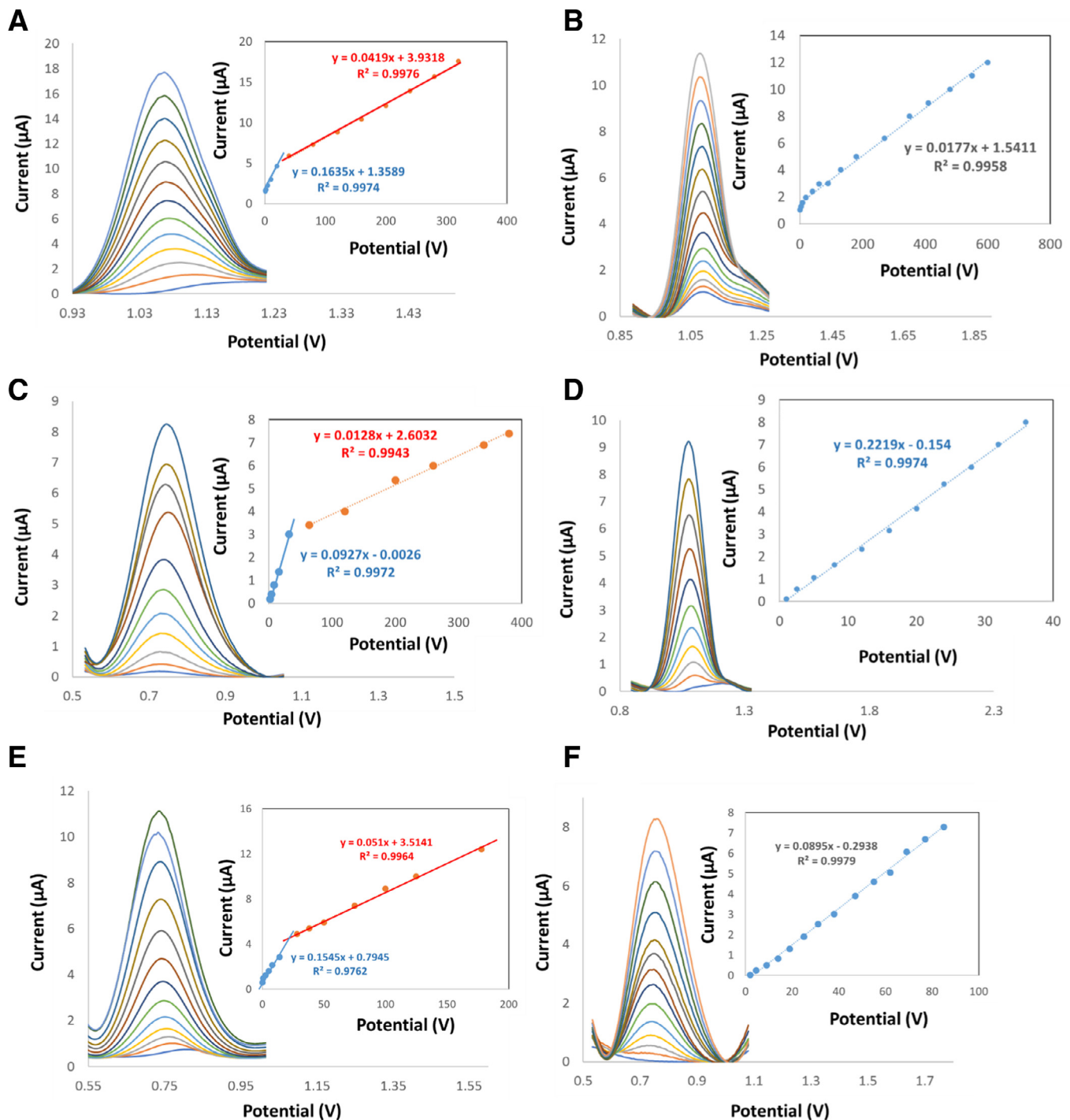


Fig. 3. Representative DPVs of (A) LDP, (B) CDP, (C) MDP, (D) BA, (E) TOL and (F) ENT in PBS (0.05 M, pH=2) at different concentrations. Insets are showing the dependence of  $I_p$  with concentration.

of interest to be calibrated, was considered and pure voltammograms of the components were used for initializing the algorithm. Finally, the algorithm was run under non-negativity of concentration and voltammetric profiles and unimodality of voltammetric profiles as applied constraints. After obtaining the single analytes' profiles, pseudo-univariate graphs were constructed by developing regression models where the area under the profile is proportional to component concentration [21]. The results of the application of the optimized model to predict concentration of the drugs in validation set are presented in Table 2. As can be seen, predictive ability of the developed model is very good for all the drugs.

After checking the predictive ability of the developed in the absence of DPA, the model performance must be verified for predicting drugs' concentrations in the presence of DPA as well. Therefore, the model was applied to the test set in which DPA was injected to the solutions with random and high concentrations. MCR-ALS was run on the test samples with the same constraints used for validation set and seven components was determined by the use of SVD. Successively, the performance of MCR-ALS to predict concentrations of the studied drugs in test set was very acceptable as can be seen in Table 2.

**Table 2**  
Predicted and nominal concentrations ( $\mu\text{M}$ ) of the studied drugs in validation and test sets by MCR-ALS and PARAFAC2.

Validation set																		
LDP Nominal	MCR-ALS Predicted	PARAFAC2 Predicted	CDP Nominal	MCR-ALS Predicted	PARAFAC2 Predicted	MDP Nominal	MCR-ALS Predicted	PARAFAC2 Predicted	BA Nominal	MCR-ALS Predicted	PARAFAC2 Predicted	TOL Nominal	MCR-ALS Predicted	PARAFAC2 Predicted	ENT Nominal	MCR-ALS Predicted	PARAFAC2 Predicted	
260	261	264	15	14.9	15.6	55	55.1	56	20	20.1	21.5	5.5	5.6	5.9	50	50.3	52.1	
300	298	304.5	24	23.8	24.9	60	60.3	61.4	12	12	11.1	24	24	25.9	45	45.1	47.3	
180	178.5	185.7	150	152.1	154	45	45	44	10	9.8	10.6	33	32.8	35	21	21	22.6	
11	11.1	10.1	121	120.4	118.9	33	32.6	31.5	5	5	5.3	12	12.1	10.5	11	11.2	13	
20	19.7	18.8	133	134	134.7	21	21.2	22	8	8.1	8.4	6	6	6.6	31	31.1	34	
6	5.9	6.4	90	90.5	92	42	42.4	44	15	14.9	15.5	66	66.5	68.1	12	11.9	11.5	
244	245.2	247	85	85.3	87	31	31	29.5	22	22	21.1	75	75.7	78.9	8.6	8.7	8	
310	308.4	316.4	54	53.6	55	29	29.3	27.7	5	5	5.2	9	9.1	9.7	25	25	23.1	
180	182.1	176	33	33.2	31.8	23	23.1	24	28	28.2	29.6	3.5	3.5	4	41	40.5	44.3	
100	101.1	97.2	22	22.1	23.1	35	34.7	36.4	11	11	12.3	18	18.2	19.6	50	50.2	52.5	
Test set																		
LDP Nominal	MCR-ALS Predicted	PARAFAC2 Predicted	CDP Nominal	MCR-ALS Predicted	PARAFAC2 Predicted	MDP Nominal	MCR-ALS Predicted	PARAFAC2 Predicted	BA Nominal	MCR-ALS Predicted	PARAFAC2 Predicted	TOL Nominal	MCR-ALS Predicted	PARAFAC2 Predicted	ENT Nominal	MCR-ALS Predicted	PARAFAC2 Predicted	
98	98.3	100.1	50	50.2	51.8	60	60.7	63.9	35	35.2	37.3	41	41.3	44.5	15	15.1	16.2	
88	88.1	92	80	80.2	82	58	58.1	64	20	20	24	29	28.8	33	25	25.5	28	
77	77	74	90	90.3	86.7	45	44.5	51	18	18.4	16.1	54	54.2	50	31	31	36	
200	201	195	100	100	106.9	54	54.4	52.1	22	22.7	19.5	4.6	4.6	4	28	28.1	22	
300	300	306.5	149	150.1	161	33	32.8	30.1	34	35	32	11	11	12.3	55	54.5	48	
210	211.4	214.5	54	54.3	57.9	22	22.6	20	30	30.6	27.1	38	38.3	39.9	44	44	51	
220	220	224	33	33	36.3	50	50	54.9	15	14.4	16.3	80	81	83	21	21.6	26	
280	281.4	275	22	22.1	24.8	48	48	52.6	10	10.2	10.4	20	20.5	24	18	18.2	12.8	
144	145	141	79	80	75	31	31.1	35.8	8	8	8.8	10	10	10.9	43	43	49.5	
233	233	229.4	88	87.3	83	30	30.4	35	14	13.6	15.3	5	5.1	6	53	54	60.8	

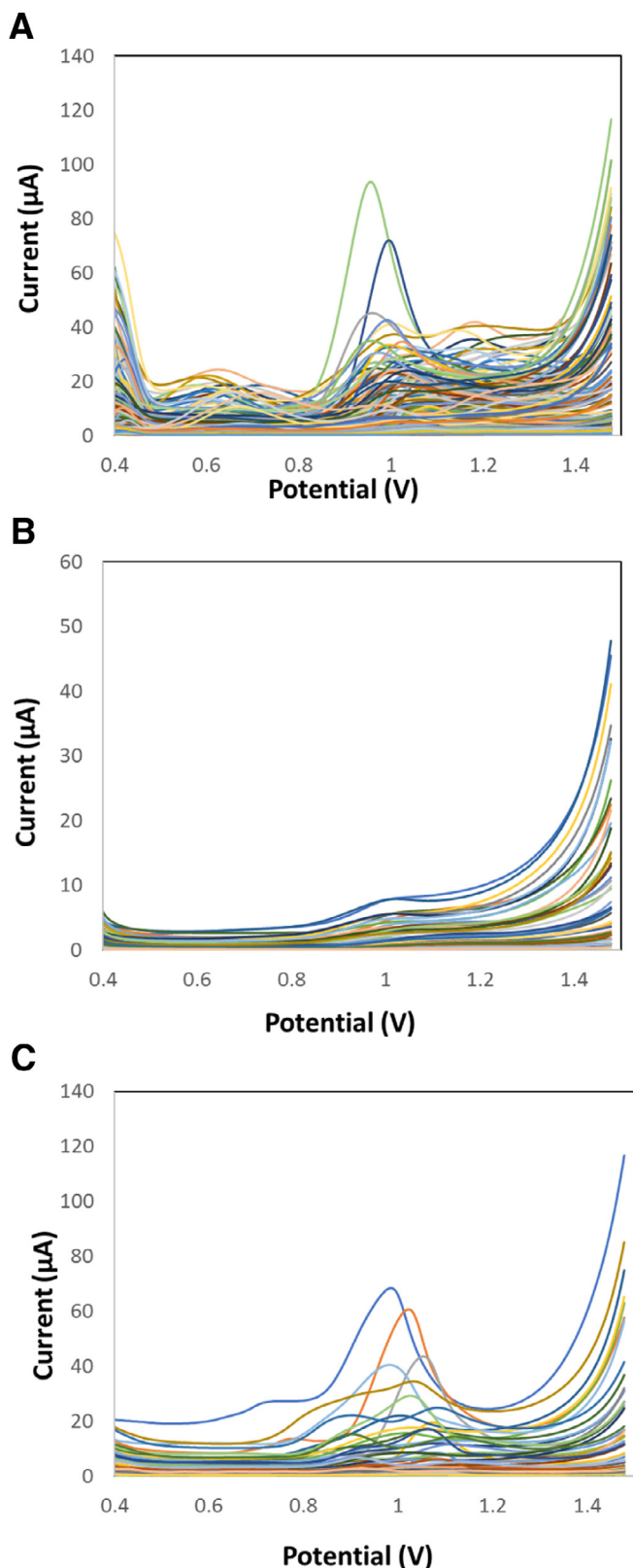


Fig. 4. Raw voltammograms: (A) calibration set, (B) validation set and (C) test set.

### 3.3.2. PARAFAC2 modeling

PARAFAC2 was also applied to build a calibration model for predicting concentrations of LDP, CDP, MDP, BA, TOL and ENT in validation and test samples. The pretreated second-order DPV data were collected into a three-way data array having dimensionality  $33 \times 5 \times 175$ , 33 calibration samples, 5 pulse heights and 175

potentials. At the first step, the PARAFAC2 model with six components was fitted to the data. Then, individual PARAFAC2 models were built each time by including one of the validation or test samples in the array. Proper number of factors was selected. In this work, the correct number of factors for each sample was determined by calculating the explained variance of the model. Voltammograms of the drugs were used in the initialization stage and non-negativity constraint was applied to concentrations and voltammograms. The obtained PARAFAC2 model didn't show a good performance in predicting concentrations of the validation set samples, as shown in Table 2. As can be seen, there are significant differences between nominal and predicted concentrations which show the inefficiency of PARAFAC2 in predicting drugs concentrations in validation set. In order to verify the prediction ability of PARAFAC2 in the presence of DPA as uncalibrated interference, it was also applied to the test set and its results are showing in Table 2. As can be seen, PARAFAC2 was not successful in the analysis of test set samples either.

### 3.4. Comparing predictive ability of MCR-ALS and PARAFAC2

In order to evaluate the performance of MCR-ALS and PARAFAC2, each model was validated by RMSEP and REP for prediction of the validation and test sets and results are presenting in Table 3. As can be seen, lower RMSEP and REP values were obtained for MCR-ALS than PARAFAC2 which guaranteed a better performance for MCR-ALS. The AFOMs including sensitivity, analytical sensitivity, selectivity and limit of detection for determination of LDP, CDP, MDP, BA, TOL and ENT by MCR-ALS and PARAFAC2 in validation and test sets are also presented in Table 3. As can be seen, the AFOMs confirmed that the MCR-ALS was more selective and sensitive than PARAFAC2 to predict drugs' concentrations in the absence and presence of DPA. For the sake of further evaluations of the accuracy of MCR-ALS and PARAFAC2, the predicted concentrations of both validation and test sets were regressed on the nominal concentrations (not shown). Here, an ordinary least squares (OLS) analysis of predicted concentrations versus nominal ones was applied [49]. The calculated intercept and slope were compared with their theoretically expected values (intercept = 0, slope = 1, ideal point), based on the elliptical joint confidence region (EJCR) test. Ellipses contain the ideal point confirm that the predicted and nominal concentrations do not present significant difference at the level of 95% confidence and the elliptic size denotes the precision of the analytical method, smaller size corresponds to higher precision [50]. Fig. 5A–D shows the corresponding ellipses of the EJCR analyses. As can be concluded from Fig. 5A–D, good predictions for LDP, CDP, MDP, BA, TOL and ENT in both validation and test sets were obtained by MCR-ALS which shows the accurate determination of drugs by the developed methodology.

### 3.5. Comparing the ability of MCR-ALS with HPLC-UV as reference method for the analysis of serum samples

When a new analytical methodology is developed, it is necessary to check its results with those of a well-known reference method. Regarding this important point, we expanded our study for comparing the accuracy of MCR-ALS for simultaneous determination of LDP, CDP, MDP, BA, TOL and ENT in a human serum sample with HPLC-UV as reference method. To evaluate the feasibility of MCR-ALS for exploiting second-order advantage, simultaneous quantification of the studied drugs was performed in a partially diluted human serum sample. The serum sample was partially diluted with PBS (0.05 M, pH 2) and spiked with different amounts of LDP, CDP, MDP, BA, TOL and ENT. Then, aliquots of the diluted samples were injected into the electrochemical cell. The DPV signals of the prepared samples in optimized conditions and differ-

**Table 3**

Analytical figures of merit and statistical indicators for determination of LDP, CDP, MDP, BA, TOL and ENT by MCR-ALS and PARAFAC2.

Validation set						
MCR-ALS						
Drug	SEN <sup>a</sup> ( $\mu\text{A} (\mu\text{M})^{-1}$ )	SEL <sup>b</sup>	LOD ( $\mu\text{M}$ )	ANAL SEN <sup>c</sup> ( $\mu\text{M})^{-1}$	RMSEP	REP (%)
LDP	4.1	0.83	5.11	73.41	1.3031	0.8089
CDP	5.5	0.88	12.3	88.00	0.7981	1.0978
MDP	2.9	0.79	13.1	81.21	0.2550	0.6817
BA	4.5	0.80	2.60	85.42	0.1049	0.7712
TOL	4.4	0.91	1.80	77.16	0.2915	1.1569
ENT	4.9	0.78	5.40	79.11	0.2145	0.7280
PARAFAC2						
Drug	SEN ( $\mu\text{A} (\mu\text{M})^{-1}$ )	SEL	LOD ( $\mu\text{M}$ )	ANAL SEN ( $\mu\text{M})^{-1}$	RMSEP	REP (%)
LDP	3.6	0.66	7.10	54.31	3.8072	2.3633
CDP	3.8	0.71	14.01	51.20	1.9005	2.6142
MDP	2.3	0.70	14.51	66.71	1.3457	3.5982
BA	3.1	0.73	5.11	69.54	0.9497	6.9834
TOL	3.6	0.69	3.46	55.41	1.8248	7.2414
ENT	3.5	0.75	6.78	61.23	2.1592	7.3291
Test Set						
MCR-ALS						
Drug	SEN ( $\mu\text{A} (\mu\text{M})^{-1}$ )	SEL	LOD ( $\mu\text{M}$ )	ANAL SEN ( $\mu\text{M})^{-1}$	RMSEP	REP (%)
LDP	4.3	0.88	54.61	75.64	0.7759	0.4194
CDP	4.9	0.83	11.60	91.23	0.5450	0.7315
MDP	2.5	0.80	15.05	86.03	0.3847	0.8926
BA	3.9	0.85	6.11	88.11	0.5109	2.4800
TOL	4.3	0.83	9.06	89.00	0.3899	1.3324
ENT	5.1	0.81	66.50	85.69	0.4382	1.3158
PARAFAC2						
Drug	SEN ( $\mu\text{A} (\mu\text{M})^{-1}$ )	SEL	LOD ( $\mu\text{M}$ )	ANAL SEN ( $\mu\text{M})^{-1}$	RMSEP	REP (%)
LDP	3.2	0.68	59.00	56.43	4.2411	2.2925
CDP	3.2	0.65	13.19	55.01	5.3355	7.1618
MDP	2.1	0.72	18.40	58.71	4.4322	10.2834
BA	2.8	0.70	10.76	61.21	2.1849	10.6065
TOL	3.3	0.69	11.80	59.06	2.7698	9.4663
ENT	3.1	0.71	68.10	52.31	5.6971	17.1084

<sup>a</sup> Sensitivity.<sup>b</sup> Selectivity.<sup>c</sup> Analytical Sensitivity.**Table 4**

Results of the analysis of human serum sample by MCR-ALS and reference method (HPLC-UV).

Opium alkaloid	MCR-ALS			Reference method (HPLC-UV)	
	Added ( $\mu\text{M}$ )	Found ( $\mu\text{M}$ )	Recovery (%)	Found ( $\mu\text{M}$ )	Recovery (%)
LDP	None	N.D <sup>a</sup>	–	N.D	–
	5	5.02	100.4	5.00	100
	28	27.8	99.3	28.06	100.2
CDP	150	151.2	100.8	150.5	100.33
	None	N.D	–	N.D	–
	200	200	100	200	100
MDP	54	53.8	99.6	54	100
	10	10.15	101.5	10	100
	None	N.D	–	N.D	–
BA	5	4.9	98	5.1	101.1
	100	102.3	102.2	101.2	101.2
	50	53.1	105.8	53.04	100.7
TOL	None	N.D	–	N.D	–
	3	3.1	103.2	3.01	100.3
	20	20.3	101.5	20.2	100.1
ENT	30	29.7	99	30.3	100.1
	None	N.D	–	N.D	–
	4	4.1	102.4	4.1	102.4
ENT	50	50.3	100.6	50.2	100.4
	100	100.5	100.5	100	100
	None	N.D	–	N.D	–
ENT	10	9.5	95	10.2	101.9
	50	48.7	99.4	50.5	100.9
	40	41.2	102.9	41.1	102.7

<sup>a</sup> Not detected.

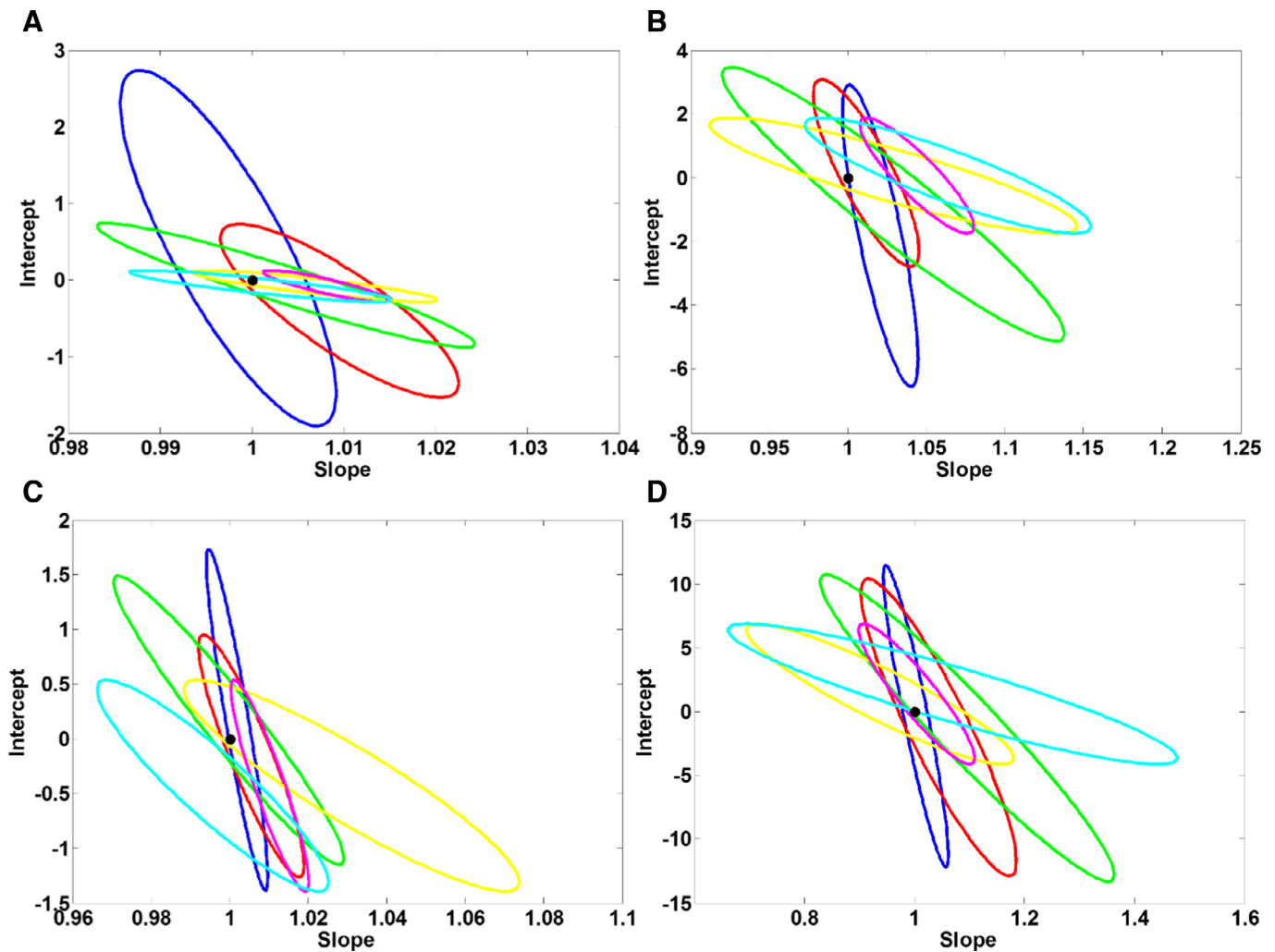


**Fig. 5.** Elliptical joint regions (at 95% confidence level) for the slopes and intercepts of the regressions: (A) MCR-ALS, validation set, (B) PARAFAC2, validation set, (C) MCR-ALS, test set and (D) PARAFAC2, test set. LDP (blue ellipse), CDP (red ellipse), MDP (green ellipse), BA (yellow ellipse), TOL (maroon ellipse) and ENT (cyan ellipse). Black point marks the ideal point (0,1). (For interpretation of the references to color in this figure legend, the reader is referred to the web version of this article.)

ent pulse heights (0.2, 0.15, 0.10, 0.05 and 0.025 V) were recorded at the GE. Table 4 presents the results obtained by the MCR-ALS with those obtained by HPLC-UV. The recovery rates for MCR-ALS results were achieved between 95% and 103.2%, showing that the blood serum matrix does not show any significant interference in simultaneous determination of LDP, CDP, MDP, BA, TOL and ENT. Although, the results indicate that the accuracy of the reference method is slightly better than that of the MCR-ALS but, it must be noted that the results obtained by MCR-ALS are in an acceptable agreement with those of obtained by HPLC-UV.

Taking into account that the acceptable results were obtained by MCR-ALS and HPLC-UV methods, either of them can be recommended for the simultaneous determination of LDP, CDP, MDP, BA, TOL and ENT in serum samples. Recommendation of the MCR-ALS depends on the analyst's knowledge about the theoretical considerations on the chemometric methods. If the analyst suffers from instrumental limitations for applying HPLC-UV, it is better to use the proposed method. However, this option needs having a background about the theoretical aspects of chemometric methods.

#### 4. Conclusions

This work reports developing an attractive electroanalytical methodology for simultaneous determination of six anti-Parkinson drugs including LDP, CDP, MDP, BA, TOL and ENT in the presence of DPA as uncalibrated interference at the surface of a gold elec-

trode with the help of three-way multivariate calibration. The six studied drugs exhibited a strong voltammetric overlapping which was successfully resolved. Two second-order algorithms including PARAFAC2 and MCR-ALS were used to model building and MCR-ALS was more successful than PARAFAC2 in predicting drugs' concentrations. Therefore, MCR-ALS was applied to the analysis of serum samples as real cases. Because of the non-bilinear behavior of voltammetric data, the COW algorithm was chosen as an efficient chemometric algorithm to tackle the non-linearity of voltammetric data. The baseline of the DPV signals was successfully removed by AsLSSR as an efficient chemometric algorithm. Finally, the application of the developed electroanalytical methodology to simultaneously assay the concentrations of LDP, CDP, MDP, BA, TOL and ENT in human serum samples allowed us to obtain satisfactory results which were in an excellent accordance with the HPLC-UV as reference method. The potential advantages of the developed method in this study such as sensitivity, rapidity and low-cost allow one to propose the present method as a promissory, cheap and accessible alternative for routine determination of the concentrations of LDP, CDP, MDP, BA, TOL and ENT in human serum samples.

#### Acknowledgments

The authors wish to express their sincere appreciation to research council of Kermanshah University of Medical sciences for financial supports of this project.

## References

- [1] Kalia LV, Lang AE. Parkinson's disease. *Lancet* 2015;386:896–912.
- [2] Sharafzadeh S, Nezamzadeh-Ejhiieh A. Using of anionic adsorption property of a surfactant modified clinoptilolite nano-particles in modification of carbon paste electrode as effective ingredient for determination of anionic ascorbic acid species in presence of cationic dopamine species. *Electrochim Acta* 2015;184:371–80.
- [3] Gilbert JA, Frederick LM, Ames MM. The aromatic-L-amino acid decarboxylase inhibitor carbidopa is selectively cytotoxic to human pulmonary carcinoid and small cell lung carcinoma cells. *Clin Cancer Res* 2000;6:4365–72.
- [4] Beers MF, Stern M, Hurlig H, Melvin G, Scarpa A. Simultaneous determination of L-dopa and 3-O-methyldopa in human serum by high-performance liquid chromatography. *J Chromatogr A* 1984;336:380–4.
- [5] Fahn S. "On-off" phenomenon with levodopa therapy in parkinsonism. *Clinical and pharmacologic correlations and the effect of intramuscular pyridoxine*. *Neurology* 1974;24:431–41.
- [6] NS Sharpless, Muentner MD, Tyce GM, Owen Jr CA. 3-Methoxy-4-hydroxyphenylalanine (3-O-methyldopa) in plasma during oral L-dopa therapy of patients with Parkinson's disease. *Clinica Chimica Acta* 1972;37(1972):359–69.
- [7] Rivera-Caiimlim E, Tandon D, Anderson F, Joynt R. The clinical picture and plasma levodopa metabolite profile of parkinsonian nonresponders. Treatment with levodopa and decarboxylase inhibitor. *Arch Neurol* 1977;34:228–32.
- [8] Shen H, Kannari K, Yamato H, Arai A, Matsunaga M. Effects of benserazide on L-DOPA-derived extracellular dopamine levels and aromatic L-amino acid decarboxylase activity in the striatum of 6-hydroxydopamine-lesioned rats. *Tohoku J Exp Med* 2003;199:149–59.
- [9] Antonini A, Abbruzzese G, Barone P, Bonuccelli U, Lopiano L, Onofri M, Zappia M, Quattrone A. COMT inhibition with tolcapone in the treatment algorithm of patients with Parkinson's disease (PD): relevance for motor and non-motor features. *Neuropsychiatr Dis Treat* 2008;4:1–9.
- [10] Chong BS, Mersfelder TL. Entacapone. *Ann Pharmacother* 2000;34:1056–65.
- [11] Ho CN, Christian GD, Davidson ER. Application of the method of rank annihilation to quantitative analyses of multicomponent fluorescence data from the video fluorometer. *Anal Chem* 1978;50:1108–13.
- [12] Booksh KS, Kowalski BR. Theory of analytical chemistry. *Anal Chem* 1994;66:782–91.
- [13] Olivieri AC. Analytical advantages of multivariate data processing. One, two, three, infinity? *Anal Chem* 2008;80:5713–20.
- [14] Arancibia JA, Damiani PC, Escandar GM, Ibañez GA, Olivieri AC. A review on second- and third-order multivariate calibration applied to chromatographic data. *J Chromatogr B* 2012;910:22–30.
- [15] Madrakian T, Afkhami A, Mohammadnejad M. Second-order advantage applied to simultaneous spectrofluorimetric determination of paracetamol and mefenamic acid in urine samples. *Anal Chim Acta* 2009;645:25–9.
- [16] Zhang Y, Wu HL, Xia AL, Han QJ, Cui H, Yu RQ. Interference-free determination of Sudan dyes in chilli foods using second-order calibration algorithms coupled with HPLC-DAD. *Talanta* 2007;72:926–31.
- [17] Edelmann A, Diewok J, Baena JR, Lendl B. High-performance liquid chromatography with diamond ATR-FTIR detection for the determination of carbohydrates, alcohols and organic acids in red wine. *Anal Bioanal Chem* 2003;376:92–7.
- [18] Pere-Trepal E, Tauler R. Analysis of environmental samples by application of multivariate curve resolution on fused high-performance liquid chromatography-diode array detection mass spectrometry data. *J Chromatogr A* 2006;1131:85–96.
- [19] Checa A, Oliver R, Saurina J, Hernandez-Cassou S. Flow-injection spectrophotometric determination of reverse transcriptase inhibitors used for acquired immunodeficiency syndrome (AIDS) treatment: focus on strategies for dealing with the background components. *Anal Chim Acta* 2006;572:155–64.
- [20] Culzoni MJ, Damiani PC, Garcia-Reiriz A, Goicoechea HC, Olivieri AC. Multi-way partial least-squares coupled to residual trilinearization: a genuine multi-dimensional tool for the study of third-order data. Simultaneous analysis of procaine and its metabolite p-aminobenzoic acid in equine serum. *Analyst* 2007;132:654–63.
- [21] Goicoechea HC, Olivieri AC. New robust bilinear least squares method for the analysis of spectral-pH matrix data. *Appl Spectrosc* 2005;59:926–33.
- [22] Nosuhi M, Nezamzadeh-Ejhiieh A. High catalytic activity of Fe(II)-clinoptilolite nanoparticules for indirect voltammetric determination of dichromate: experimental design by response surface methodology (RSM). *Electrochim Acta* 2017;223:47–62.
- [23] Nosuhi M, Nezamzadeh-Ejhiieh A. Comprehensive study on the electrocatalytic effect of copper-doped nano-clinoptilolite towards amoxicillin at the modified carbon paste electrode-solution interface. *J Colloid Interface Sci* 2017;497:66–72.
- [24] Amani-Beni Z, Nezamzadeh-Ejhiieh A. A novel non-enzymatic glucose sensor based on the modification of carbon paste electrode with CuO nanoflower: designing the experiments by response surface methodology (RSM). *J Colloid Interface Sci* 2017;504:186–96.
- [25] Nezamzadeh-Ejhiieh A, Shahanshahi M. Modification of clinoptilolite nano-particles with hexadecylpyridinium bromide surfactant as an active component of Cr(VI) selective electrode. *J Ind Eng Chem* 2013;19:2026–33.
- [26] Sharifian S, Nezamzadeh-Ejhiieh A. Modification of carbon paste electrode with Fe(III)-clinoptilolite nano-particles for simultaneous voltammetric determination of acetaminophen and ascorbic acid. *Mater Sci Eng C* 2016;58:510–20.
- [27] Saadat M, Nezamzadeh-Ejhiieh A. Clinoptilolite nanoparticles containing HDTMA and Arsenazo III as a sensitive carbon paste electrode modifier for indirect voltammetric measurement of Cesium ions. *Electrochim. Acta* 2016;217:163–70.
- [28] Nosuhi M, Nezamzadeh-Ejhiieh A. An indirect application aspect of zeolite modified electrodes for voltammetric determination of iodate. *J Electroanal Chem* 2018;810:119–28.
- [29] Gholivand MB, Jalalvand AR, Goicoechea HC, Skov T. Chemometrics-assisted simultaneous voltammetric determination of ascorbic acid, uric acid, dopamine and nitrite: application of non-bilinear voltammetric data for exploiting first-order advantage. *Talanta* 2014;119:553–63.
- [30] Gholivand MB, Jalalvand AR, Goicoechea HC, Gargallo R, Skov T, Paimard G. Combination of electrochemistry with chemometrics to introduce an efficient analytical method for simultaneous quantification of five opium alkaloids in complex matrices. *Talanta* 2015;131:26–37.
- [31] Gholivand MB, Jalalvand AR, Goicoechea HC, Skov T. Generation of non-multilinear three-way voltammetric arrays by an electrochemically oxidized glassy carbon electrode as an efficient electronic device to achieving second-order advantage: challenges, and tailored applications. *Talanta* 2015;134:607–18.
- [32] Jalalvand AR, Gholivand MB, Goicoechea HC, Rinnan A, Skov T. Advanced and tailored applications of an efficient electrochemical approach assisted by AsLSSR-COW-rPLS and finding ways to cope with challenges arising from the nature of voltammetric data. *Chemom Intell Lab Syst* 2015;146:437–46.
- [33] Jalalvand AR, Gholivand M-B, Goicoechea HC. Multi-dimensional voltammetry: four-way multivariate calibration with third-order differential pulse voltammetric data for multi-analyte quantification in the presence of unexpected interferences. *Chemom Intell Lab Syst* 2015;148:60–71.
- [34] Jalalvand AR, Goicoechea HC, Rutledge DN. Applications and challenges of multi-way calibration in electrochemical analysis. *TrAC Trends Anal Chem* 2017;87:32–48.
- [35] Jalalvand AR, Goicoechea HC. Applications of electrochemical data analysis by multivariate curve resolution-alternating least squares. *TrAC Trends Anal Chem* 2017;88C:134–66.
- [36] Faulkner LR, Bard AJ. *Electrochemical methods: fundamental and application*. Second ed. New York: Wiley; 2001.
- [37] Goicoechea HC, Olivieri AC. New robust bilinear least squares method for the analysis of spectral-pH matrix data. *Appl Spectrosc* 2005;59:926–33.
- [38] R.A. Harshman, *PARAFAC2: mathematical and technical notes*, UCLA Working Papers Phonetics 22 (1972) 30–47.
- [39] Kiers HAL, ten Berge JMF, Bro R. PARAFAC2-Part I. A direct fitting algorithm for the PARAFAC2 model. *J Chemometr* 1999;13:275–94.
- [40] Bro R, Andersson CA, Kiers HAL. PARAFAC2-Part II. Modeling chromatographic data with retention time shifts. *J Chemometr* 1999;13:295–309.
- [41] Eilers PHC, Currie ID, Durban M. Fast and compact smoothing on large multi-dimensional grids. *Comput Stat Data Anal* 2006;50:61–76.
- [42] Eilers PHC. Parametric time warping. *Anal Chem* 2004;76:404–11.
- [43] Nielsen NPV, Carstensen JM, Smedsgaard J. Aligning of single and multiple wavelength chromatographic profiles for chemometric data analysis using correlation optimised warping. *J Chromatogr A* 1998;805:17–35.
- [44] Cormen TH, Leiserson CE, Rivest RL, Stein C. *Introduction to algorithms*. Cambridge, MA, USA: The MIT Press; 2001.
- [45] Tomasi G. *Practical and computational aspects in chemometric data analysis*, Frederiksberg, Denmark: The Royal Veterinary And Agricultural University; 2006. Ph.D. Dissertation.
- [46] Olivieri AC, Escandar GM. *Practical three-way calibration*. Amsterdam: Elsevier; 2014.
- [47] Suh JH, Lee YY, Lee HJ, Kang M, Hur Y, Lee SN, Yang DH, Han SB. Dispersive liquid-liquid microextraction based on solidification of floating organic droplets followed by high performance liquid chromatography for the determination of duloxetine in human plasma. *J Pharm Biomed Anal* 2013;75:214–19.
- [48] Windig W, Guilment J. Interactive self-modeling mixture analysis. *Anal Chem* 1991;63:1425–32.
- [49] Gonzalez AG, Herrador MA, Asuero AG. Intra-laboratory testing of method accuracy from recovery assays. *Talanta* 1999;48:729–36.
- [50] Arancibia JA, Escandar GM. Two different strategies for the fluorimetric determination of piroxicam in serum. *Talanta* 2003;60:1113–21.